Danilo MAKUC, Klemen DROBNIČ, Vanja AMBROŽIČ, Damijan MILJAVEC, Rastko FIŠER, Mitja NEMEC

University of Ljubljana, Faculty of Electrical Engineering

Parameters estimation of induction motor with faulty rotor

***Abstract**. This paper describes the evaluation of parameters of a three-phase induction motor with broken rotor bars. Using standard d-q model of induction motor the electric and magnetic asymmetry can be expressed through differently modified rotor parameters in both axes. A non-standard, one-phase measuring method was employed. To assess the measurement results of the method and to predict various situations which can not be achieved by measurements an extensive finite element analysis has been performed.*

Streszczenie.** Niniejszy artykuł opisuje ocenę parametrów trójfazowego silnika indukcyjnego z pękniętym prętem wirnika. Za pomocą standardowego modelu d-q silnika indukcyjnego, elektryczna i magnetyczna asymetria może być wyrażona przez inne zmodyfikowane parametry wirnika w obu osiach. Zastosowana została niestandardowa, jednofazowa metoda pomiaru. W celu oceny wyników pomiarów metody i zapobiegania różnym sytuacjom niemożliwym do zmierzenia zastosowano obszerną analizę elementów skończonych. (**Estymacja parametrów silnika indukcyjnego z uszkodzonym wirnikiem)

Keywords: Broken rotor bars, Induction machines, Parameter measurement.
Słowa kluczowe: pęknięty pręt wirnika, maszyna indukcyjna, pomiar parametrów.

Introduction

Equivalent circuit model constitutes a basic, yet sufficiently general mathematical description of induction motor and is derived directly from a corresponding transformer model. The rotor side quantities, which include rotor current, leakage reactance and resistance, are referred to stator by a coil ratio. A few variants are known, of which basic T-model is the most usual choice [1]. Nowadays, a number of complex models are also available, often combining magnetic field theory with classic circuit approach which can now easily deal with once "hard-to-calculate" effects of induction machine, such as magnetic saturation, iron losses, etc [2].

Appearance of broken rotor bars in induction machine gives rise to some well-known phenomena discernible in electric and mechanic quantities [3]. Typical approach to embrace the effects of this specific fault is to model internal state of the machine with sufficient precision. Therefore, finite element analysis (FEA) [4] or models with high-number of differential equations [5, 6] have been used for simulations yielding very accurate results and taking into account even less tangible, second order effects. For example, in [7] it has been shown how the redistribution of the current in rotor bars amplifies local saturations which in turn decrease the expression of the fault on stator current. Obvious drawback of these advanced approaches is rather high computational burden and often machine-specific model.

Recently introduced two-axis model of induction machine with broken rotor bars [8] equals the former approaches in purpose but differs in fundamental approach. Model is based on the assumption that broken bar can be described as some sort of salience of a squirrel cage resulting in different rotor parameters in *d*-, and *q*-axes, respectively. Consequently, measured from the stator side, these parameters will vary with the rotor angle [9].

Accuracy of this model clearly depends on the exactness of parameters, which must be determined beforehand. Standard induction motor tests as no-load, rated load and short-circuit, which are designed for symmetrical rotor, cannot take into account rotor saliency and must therefore be replaced with measurements capable of establishing proper relationship between rotor angle and machine parameters. In this paper, an evolution of a method for determining angle-dependent rotor parameters, is presented. Induction motor is supplied only with one phase voltage while keeping the rotor locked. By changing alignment of rotor in respect to stator magnetic axis, dependence of the machine parameters on rotor angle can be obtained.

Independently from measurements, the machine parameters were computed using FEA of the very same induction motor with faulty rotor. On one hand, FEA provides a verifying tool for the measurements, but it also allows a study many of different cases and combinations of rotor faults for which measurements are difficult to perform due to the limited test hardware. Additionally, dependence of rotor parameters on frequency was also dealt with, taking into account skin-effect and local magnetic saturations of the iron core.

Induction Motor Model

The model of induction motor with broken bars is derived directly from a classic two-phase *d-q* model depicted in Fig.1. Its obvious advantage is that solely two voltage equations are necessary to describe electromagnetic phenomena in the machine. One of the prerequisites that concede the use of this model is machine's internal electrical symmetry, which translates itself to symmetrical stator windings and rotor cage [10, 11].

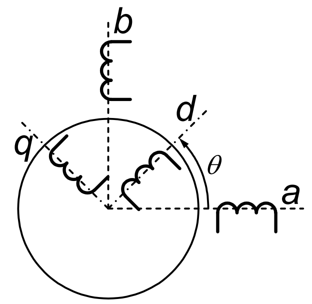

Fig. 1. Two-phase model of induction motor.

With the onset of rotor fault in form of broken or cracked bars internal symmetry becomes distorted. At this point the classic *d-q* model needs to be reevaluated and adjusted to new conditions. Question whether Park transformation, essential for derivation of *d-q* model, is still valid despite rotor asymmetry has been dealt with in [8]. Namely, the occurrence of fault modifies rotor parameters in a certain way. It was shown in [8] that rotor resistance and inductance change depending on rotor position (i.e. its electrical angle) following sinusoidal shape. In this way, the transformation remains valid with electrical asymmetry taken into account.

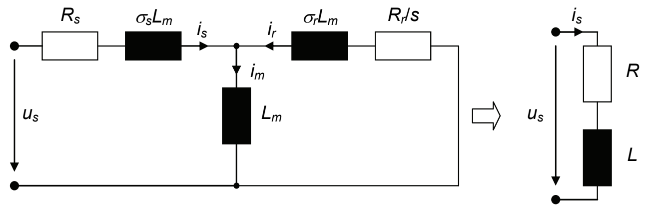

Fig. 2. Single phase equivalent circuit of induction machine.

In order to benefit from this simple yet satisfactory accurate model, its parameters must be ascertained. A starting point for the analysis is an induction machine single phase equivalent circuit (Fig. 2). Following established test procedure for induction motor using no-load and short-circuit test, the parameters of the machine can be determined. At no-load, when a slip value s is practically zero, all of the stator current flows through the magnetizing inductance thus substitute inductance equals $L = \sigma_s L_m + L_m$ and substitute resistance $R = R_s$. In a short-circuit state (locked rotor) the slip equals one and most of the current flows through the rotor branch thus $L = \sigma_s L_m + \sigma_r L_m$ and $R = R_s + R_r$.

Since the rotor with broken rotor bars exhibits electrical asymmetry, measurement in a rotating magnetic field or with a rotating rotor in a stationary field cannot yield the dependence of machine parameters on rotor angle. The only way to obtain the parameters of the asymmetrical machine is with locked rotor and a stationary sinusoidal pulsating magnetic field [9]. The stator windings are supplied with one phase voltage only, where rotor angle θ is defined as the angle between the axis of stator field and the axis of rotor fault. Measurement of the parameters at different orientations of the rotor regarding the stator field should give the dependence of the parameters on the rotor position (Fig. 3).

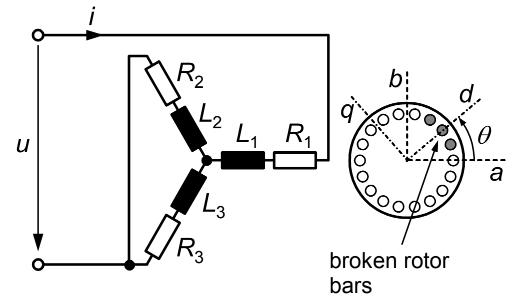

Fig. 3. Single phase measurement of machine parameters at standstill (assuming 2-pole machine).

However, machine parameters cannot be considered as constant. As it was already pointed out, the rotor resistance and inductance change duly with respect to rotor position. Additionally, machine is influenced by some other more or less pronounced effects. For example, with growing supply frequency rotor bars are subject to “skin-effect”, which can seriously hamper accurate determination of rotor resistance [12]. In order to take account of this particular phenomenon, frequency dependence of machine parameters has to be evaluated as well.

Being the machine short-circuited, the supply frequency corresponds to the slip s = 1. However, the maximum reasonable frequency (at pull-out slip) is to low to presume the absence of a magnetizing inductance as stated before. Therefore, parameters have to be measured at various frequencies thus emulating real no-load and short-circuit condition. Which frequency should be considered to correspond to the virtual short-circuit (enabling to presume $R = R_s + R_r$) is hard to say, especially considering the above mentioned parasite effects and non-linearities. To demonstrate these phenomena, let us observe substitute resistance and inductance just for a healthy rotor obtained from measurements and FEA at different frequencies (Fig. 4). Obviously, at high frequency, as the substitute resistance in simulation tends to stabilize, the actual measurement show different behavior. It is the goal of this paper to analyze and explain these parasitic effects influencing parameter estimation, thus helping to obtain more accurate models for parameter estimation as demanded in [9].

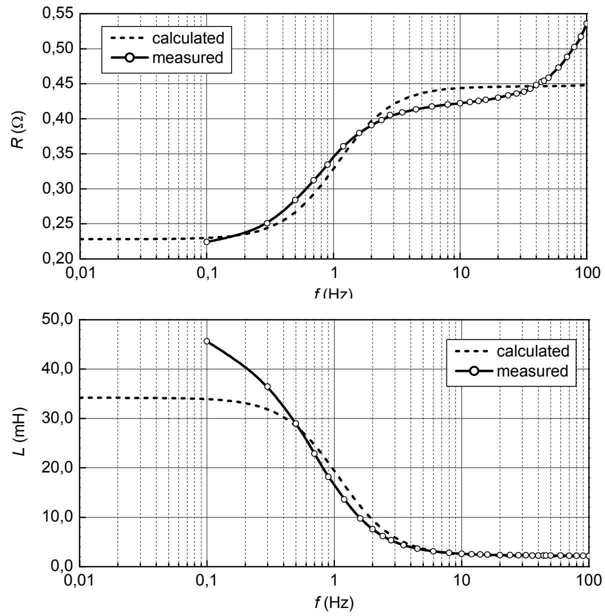

Fig. 4. Frequency dependence of machine parameters for single phase measurement and FEA for a healthy rotor at standstill.

In presented analysis two rotors were considered. Apart from healthy one (no broken bars), a rotor with 7 broken bars out of 44 (as being the only available), was used and is subsequently referred as “faulty”.

Calculations Using FEA

Using a 2D FEA, a case study of different rotor asymmetries due to broken rotor bars was considered and machine parameters were calculated at different rotor angles. Results of FEA were used for comparison with measured data and to compute parameters or investigate the operating conditions that cannot be realized or measured on a real induction machine. Broken rotor bars were modeled as non-conducting bars in a squirrel cage where all bars are connected in parallel.

Due to a 2D model the stray inductances of windings' heads were neglected. A frequency domain solver was used to analyze this configuration, while stator windings were supplied by the same current values as in measurements.

Computations of Motor Parameters at Lower Frequencies

At low supply frequencies (below 1 Hz) the induced currents in rotor winding (bars) are also low and stator current consists mainly of magnetizing current. The influence of short circuited rotor winding on the shape and magnitude of the magnetic field in the machine is very weak. Flux lines at different rotor (fault) positions, at supply frequency of 0.1 Hz, are shown in Fig. 5. As expected, the shape of the magnetic field is not influenced by rotor position. Furthermore, the field would almost be the same if there were no conducting bars in rotor slots at all. Although in this case the rotor cage has seven broken bars (in order to make FEA more pronounced), there is just a negligible difference when the position of the fault is rotated from direct (Fig. 5a) to quadrature axis (Fig. 5b). Even though the absence of seven rotor bars produces current asymmetry in the rotor, the magnetizing current (through L_m) in such case is much higher.

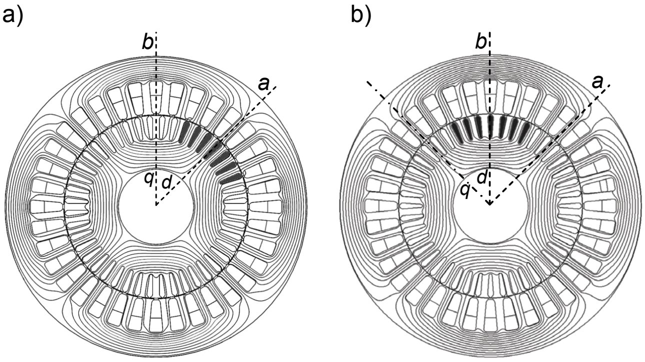

Fig. 5. Magnetic field in induction machine with 7 broken rotor bars supplied by a single phase voltage at 0.1 Hz, when broken rotor bars are in (a) direct axis and (b) quadrature axis.

To get a complete dependence of a substitute resistance R and inductance L on healthy and faulty rotor due to rotor angle (position) θ, calculations were performed for a span of 180 electrical degrees. The results are shown in Fig. 6. One can observe a slight variation of resistance depending on the position of the fault axis, while the substitute inductance ($\sigma_s L_m + L_m$) is practically constant irrespectively to rotor angle θ. It can be deduced that the total stator inductance (consisting of stator stray and magnetizing inductance) practically does not depend on the damage level of the rotor.

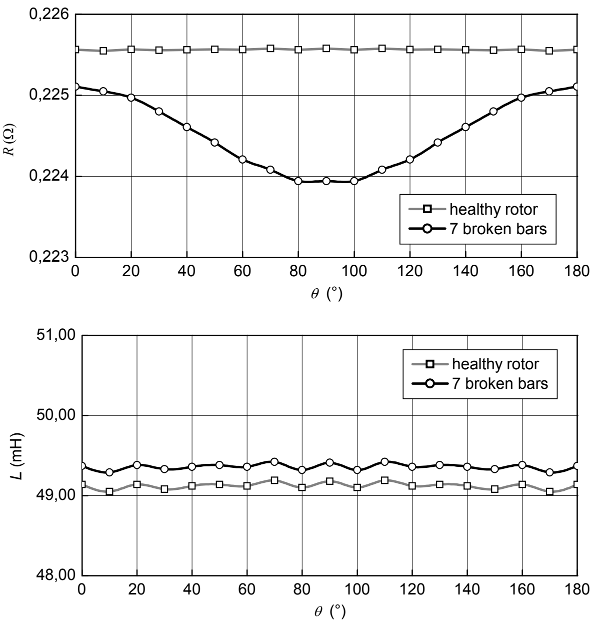

Fig. 6. Calculated resistance and inductance at 0.1 Hz versus rotor position for healthy rotor and rotor with 7 broken rotor bars.

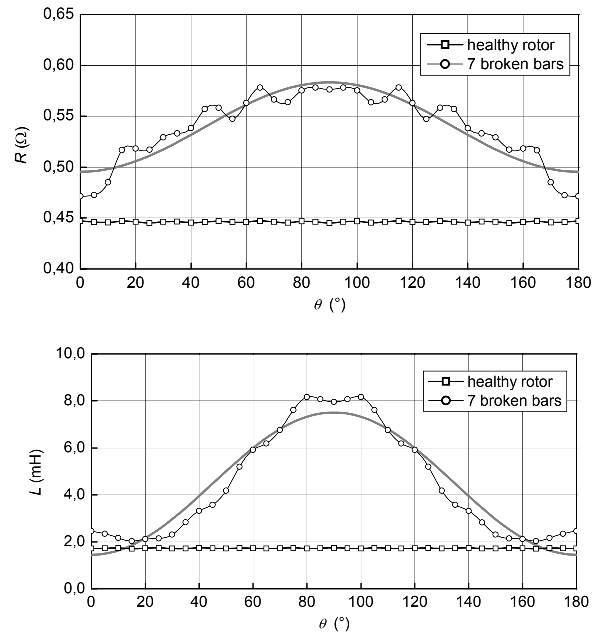

Fig. 7. Calculated resistance and inductance at 100 Hz versus rotor position for healthy rotor and rotor with 7 broken rotor bars.

Computations of Motor Parameters at Higher Frequencies

At frequencies above 1 Hz the impact of broken rotor bars on substitute parameters is far more accentuated, since the rotor currents are now much higher and have considerable influence on magnetic field in the machine.

Taking it to extreme, values of substitute resistance and inductance at supply frequency of 100 Hz for different rotor positions θ are shown in Fig. 7. As with a low frequency supply, results show that in case of healthy rotor both the resistance and inductance are independent on θ, while with (seven) broken rotor bars both quantities are highly dependent on rotor position. Deviations from healthy values are maximal when the fault position (rotor axis *d*) is aligned with a stator quadrature axis *b*. When the fault is aligned with a stator direct axis *a* the values almost match the healthy ones.

In this case the frequency is so high that large induced rotor currents almost compensate the stator excitation, therefore only stray magnetic field of stator and rotor windings are present in the machine. The magnetizing current in a parallel branch of equivalent circuit can easily be neglected in such circumstances (Fig. 2).

In Fig. 8 the flux lines in both utmost rotor positions are shown, where almost no flux line encloses both the stator and the rotor winding. In both figures (Fig. 8a and Fig. 8b) directions of rotor currents are indicated. It is obvious that broken bars prevent currents to flow, but it is also evident how position of rotor fault actually influences the current distribution. When the fault is aligned with a direct axis (Fig. 8a) the currents are in fact not very disturbed, since also healthy rotor has practically no current in rotor bars which are positioned close to the axis of magnetic field.

We encounter a quite opposite situation when faulty bars lie in a quadrature axis. In a healthy rotor these are exactly the bars which conduct the majority of the rotor current. In the presented case with seven broken rotor bars just two remaining bars have to conduct the whole current (Fig. 8b). That influences the raise of the substitute resistance since the cross section of two bars is considerably smaller than that of nine, which would normally conduct the current.

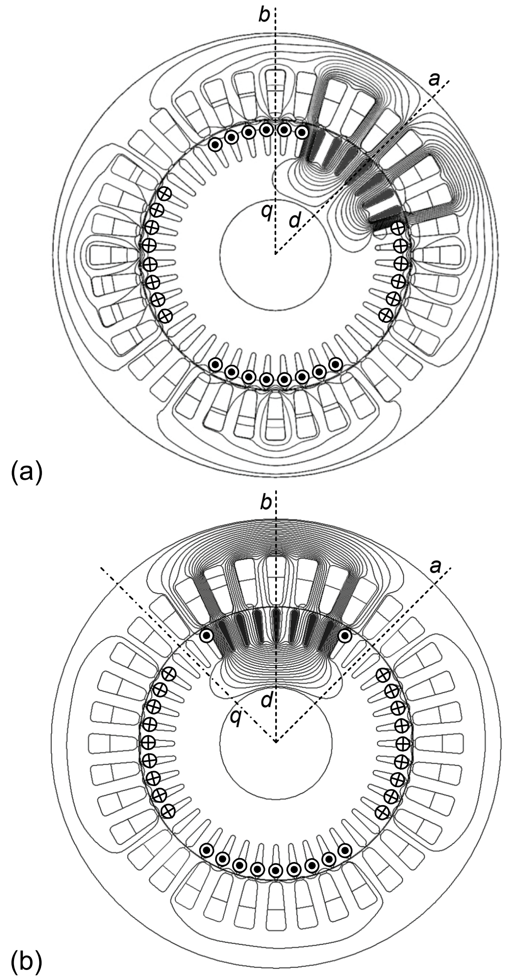

Fig. 8. Magnetic field in induction machine with 7 broken rotor bars supplied by a single phase voltage at 100 Hz when broken rotor bars are in (a) direct axis and (b) quadrature axis. In both cases directions of rotor currents are indicated.

The variation of the resistance has a sinusoidal profile with a period being half of a pole-pair period (Fig. 7). Also the minimal substitute resistance of a motor with broken rotor bars is somewhat higher than with healthy rotor, since it is evident that even in alignment of direct axis such an extended fault (7 broken bars) effects the current distribution very much.

The substitute inductance is also expectedly constant for a healthy machine and has similar sinusoidal profile as the resistance for the machine with broken rotor bars. The inductance rises due to the fact that part of the stator winding has no counter-ampere-turns and therefore the magnetic field spreads almost undisturbed into the rotor. Thus the magnetizing component of the current slightly increases which also affects the value of already small substitute inductance. Since the number of broken bars in the model is very high, this effect has also a relatively big influence on a value of a substitute inductance. In spite of that, the substitute inductance at high frequencies consists mainly of stator and rotor stray inductances ($\sigma_s L_m + \sigma_r L_m$).

The reason for the calculated resistance and inductance profile not being completely sinusoidal is the fact that, due to simplicity, a 2D FEA model was used and the effect of a skewed rotor was not taken into account. Rotor teeth and slots consequently form magnetic saliency, which influences the resultant profiles. Since the main goal was to show how and how much the rotor faults effect the motor parameters, the obtained results entirely confirm our expectations.

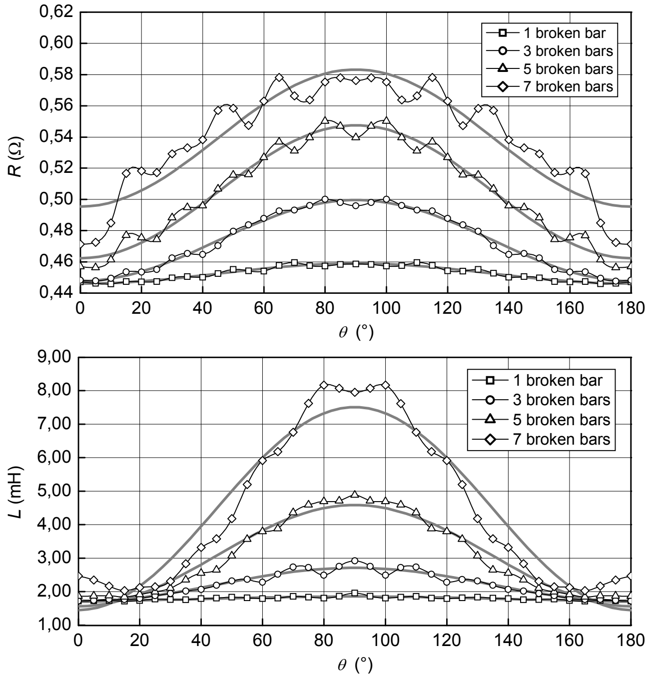

Fig. 9. Calculated resistance and inductance at 100 Hz versus rotor position for motor with 1, 3, 5 and 7 broken rotor bars.

Number of Broken Rotor Bars

The magnitude of parameter change due to rotor faults is practically defined by the number ob broken rotor bars. In this case only faults where broken bars appear in a group were analyzed by means of FEA. Results of substitute parameters for 1, 3, 5, and 7 broken bars are shown in Fig. 9. A sinusoidal approximation was used for all obtained profiles. As expected the saliency diminishes with a smaller number of broken rotor bars.

Frequency Response

To verify the assumption that values of substitute quantities at very low and very high frequencies remain almost constant, frequency response of the machine was calculated and measured in two positions – rotor fault aligned with stator axis *a* and axis *b*, respectively.

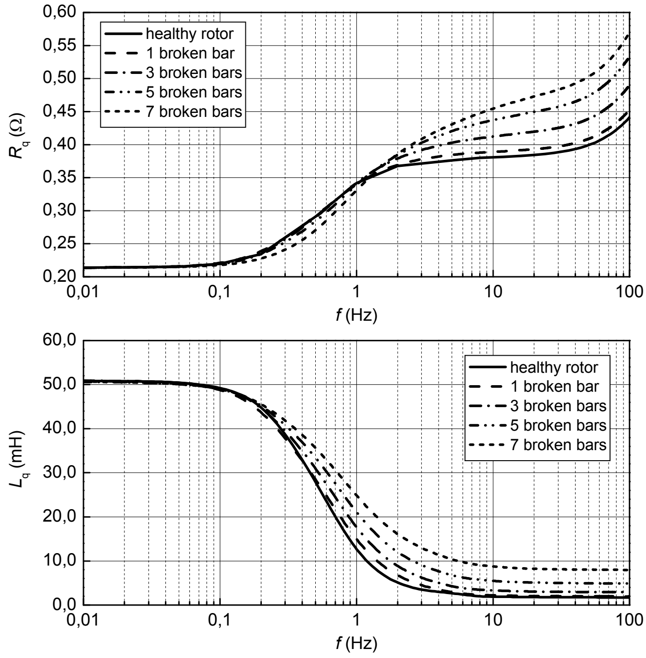

Fig. 10. Calculated frequency response of quadrature resistance and inductance for different numbers of broken rotor bars.

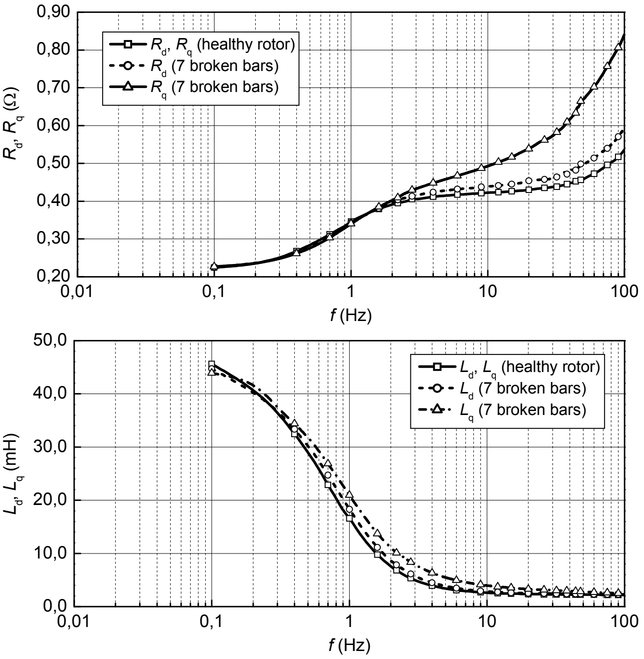

Fig. 11. Measured frequency response of direct and quadrature resistance and inductance for healthy and faulty rotor.

Simulated responses for different fault degrees (increasing number of broken bars) are presented in Fig. 10, while the measurement results are shown in Fig. 11. The latter could have been performed only for seven broken bars due to the available damaged rotor. In Fig. 10 only quadrature resistance and inductance are shown, since direct components do not show mentionable deviations from values of a healthy rotor. It can be seen that the substitute inductances start from the same value and asymptotically approach finite values at high frequency (depending on the level of fault. This is not the case with a substitute resistance. When the supply frequency rises above 20 Hz the resistance tends to increase steeply. Since the rotor bars are massive, skin effect is the main cause for such behaviour. The effect is evident with a healthy rotor as well as with broken rotor bars. This fact aggravates the simple estimation of equivalent circuit parameters.

Since there is no special need for monitoring the parameters at so high (above rated) frequency, the resistance at frequencies above 20 Hz can be approximated with a nonlinear function [12] and then extrapolated to 0 Hz, which gives a value of substitute resistance without increase caused by a skin effect. This value can be then easily distributed among stator and rotor resistance ($R_s + R_r$). In Fig. 12 the calculated frequency response of quadrature resistance with the approximation function are shown.

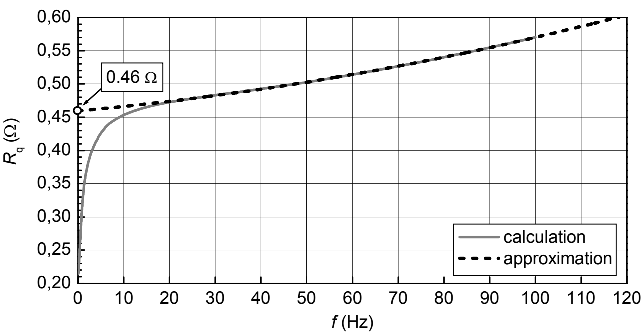

Fig. 12. Calculated frequency response of quadrature resistance for 7 broken bars and the approximation function which is extrapolated down to 0 Hz.

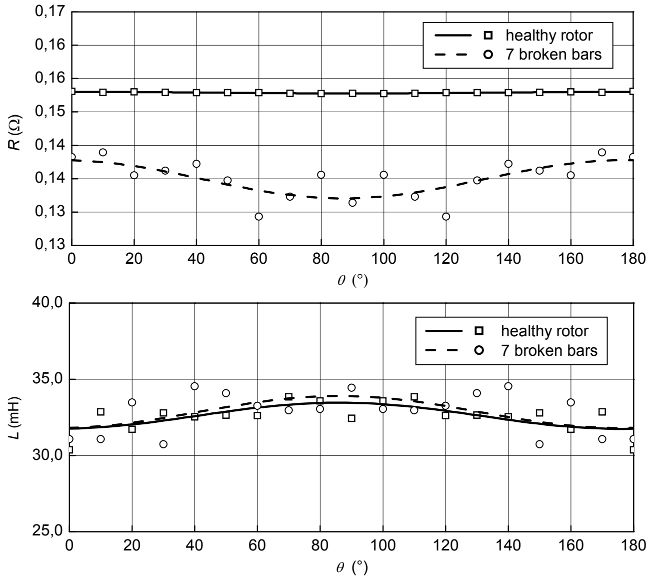

Fig. 13. Measured resistance and inductance at 0.1 Hz versus rotor position for healthy rotor and rotor with 7 broken rotor bars.

Experimental Result

Experimental measurements were made with a variable frequency voltage/current source and an oscilloscope. Measurement principle was already described in Fig. 3. Substitute resistances and inductances were calculated from phase angle between impressed phase voltage and phase current, and their amplitudes. As expected from simulation results (Fig. 6), broken rotor bars do not have significant impact at low supply frequencies (Fig. 13). Note that phase angle needed for impedance determination is hard to obtain precisely at extremely low frequencies.

At higher frequencies we can observe in Fig. 14 the same sinusoidal profile that was evident from simulations (Fig. 7). While there are some discrepancies in the offsets as well as in magnitudes between simulations and measurements, they could be attributed to simplified simulation model (only 2D simulation, no skewing of rotor bars, neglected stray inductance, …).

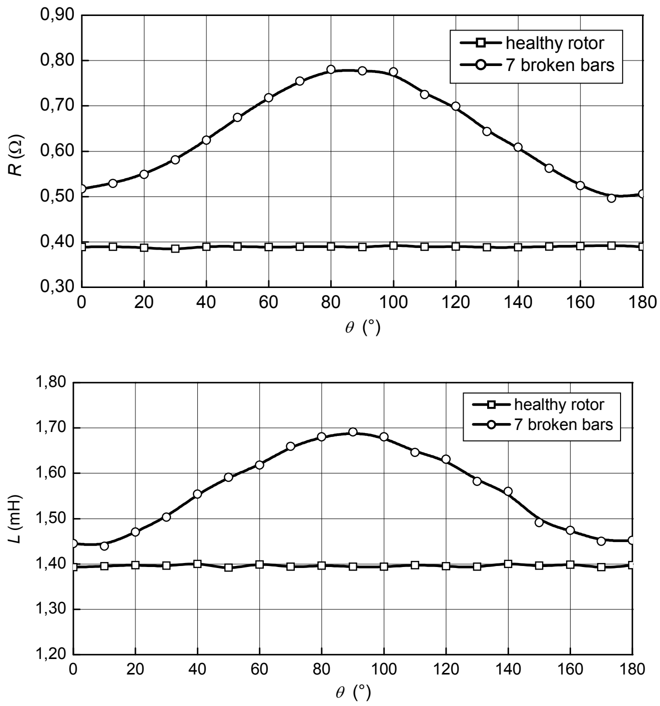

Fig.14. Measured resistance and inductance at 100 Hz versus rotor position for healthy rotor and rotor with 7 broken rotor bars.

Conclusion

In this paper, parameter variations in an induction machine with a healthy and gradually damaged rotor as well as their intrinsic nonlinearities have been investigated and explained through both FEA and measurement. In order to determine the presumed angular distribution of parameters, an already developed method using single-phase supply at different frequencies had to be adapted. By simple extrapolation of the substitute resistance frequency response the influence of skin effect present at higher supply frequencies can be mitigated, thus giving correct parameters at low frequencies.

The aim of this work is to provide parameters for a dynamic model of a faulty machine. With such a model, developed in different reference frames, dynamical behaviour of the machine could be investigated at different operating conditions and fault stages. Ultimately, this analysis offers an insight in the machine operation that could be used for diagnostic purposes or fault-tolerant operation.

Appendix

Manufacturer's data of the applied induction machine is presented in Table 1.

Table 1. Rated parameters of induction machine (healthy rotor)

P	3 kW	R_s	0.214 Ω
U_s	177 V	L_s	35.4 mH
I_s	14.8 A	R_r	0.231 Ω
n	1456 rpm	L_r	35.0 mH
T	20 Nm	L_m	34.1 mH

REFERENCES

[1] M. Stieber, "Determining induction machine parameters using equivalent circuit models," ICEM 2004, Krakow, Poland, 5-8. Sept. 2004.

[2] M. Dems, K. Komeza, "Comparison of different models for the calculation of transient processes of large power induction motors on soft and frequency start-up", ICEM 2006, Chania, Greece, 2-5 Sept. 2006.

[3] M.E.H. Benbouzid, G.B. Kliman, "What stator current processing-based technique to use for induction motor rotor faults diagnosis?," IEEE Transactions on Energy Conversion, vol.18, no.2, pp. 238- 244, June 2003.

[4] R. Fišer, D. Makuc and V. Ambrožič, "Evaluation of the induction motor cage fault stage using finite element method," SDEMPED 2001, Grado, Italy, Sept. 1-3 2001.

[5] J. Jung and B. Kwon, "Corrosion model of a rotor-bar-under-fault progress in induction motors," IEEE Transactions on Industrial Electronics, vol. 53, no. 6, pp. 1829 -1841, Dec. 2006.

[6] H. A. Toliyat and T. A. Lipo, "Transient analysis of cage induction machines under stator, rotor bar and end ring faults," IEEE Transactions on Energy Conversion, vol. 10, no. 2, pp. 241 -247, June 1995.

[7] J. Sprooten, J.C. Maun, "Influence of Saturation Level on the Effect of Broken Bars in Induction Motors Using Fundamental Electromagnetic Laws and Finite Element Simulations," IEEE Transactions on Energy Conversion, vol.24, no.3, pp.557-564, Sept. 2009.

[8] M. Nemec, D. Makuc, V. Ambrožič, and R. Fišer, "Simplified model of induction machine with electrical rotor asymmetry," ICEM 2010, Rome, Italy, 6-8 Sept. 2010.

[9] M. Nemec, V. Ambrožič, R. Fišer, and D. Makuc, "Parameters estimation using single phase measurement of three phase induction machine", Przegląd Elektrotechniczny, nr. 3/2001, pp. 129-132, March 2011.

[10] C. V. Jones. Unified theory of electrical machines, London: Butterwoths, 1967.

[11] P. C. Krause, S. D. Sudhoff, O. Wasynczuk, "Analysis of electric machinery and drive systems", New York: Wiley Interscience, 2002.

[12] A. Boglietti, A. Cavagnino, L. Ferraris, M. Lazzari, "Skin effect experimental validations of induction motor squirrel cage parameters," ICEM 2008, 6-9 Sept. 2008.

***Authors**: Danilo Makuc, E-mail: danilo.makuc@fe.uni-lj.si; Klemen Drobnič, E-mail: klemen.drobnic@fe.uni-lj.si; Vanja Ambrožič, E-mail: vanja.ambrozic@fe.uni-lj.si; Damijan Miljavec, E-mail: damijan.miljavec@fe.uni-lj.si; Rastko Fišer, E-mail: rastko.fiser@fe.uni-lj.si; Mitja Nemec, E-mail: mitja.nemec@fe.uni-lj.si. All the authors are with University of Ljubljana, Faculty of Electrical Engineering, Department of Mechatronics, Trzaska 25, 1000 Ljubljana, Slovenia.*